

Internal distortion in ceria-doped hafnia solid solutions: High-resolution x-ray diffraction and Raman scattering

Hirotaaka Fujimori,* Masatomo Yashima,† Satoshi Sasaki, and Masato Kakihana
Materials and Structures Laboratory, Tokyo Institute of Technology, Yokohama 226-8503, Japan

Takeharu Mori and Masahiko Tanaka
Photon Factory, Institute of Materials Structures Science, High Energy Accelerator Research Organization, Tsukuba 305-0801, Japan

Masahiro Yoshimura‡
Materials and Structures Laboratory, Tokyo Institute of Technology, Yokohama 226-8503, Japan
 (Received 14 July 1999; revised manuscript received 28 September 2000; published 11 September 2001)

High-resolution synchrotron x-ray powder diffraction and Raman scattering have indicated the existence of tetragonal ceria-doped hafnia with both an axial ratio c_f/a_f of unity and internal shear deformation. The values of c_f/a_f ratio in HfO_2 - X -mol % - CeO_2 samples ($X=80, 85,$ and 90) are estimated to be 1 ± 0.00004 from the estimated standard deviation of the peak positions and to be 1 ± 0.002 from the full width at half maximum of the 400_f reflection peaks. However, the Raman spectra of these samples clearly demonstrate the tetragonal phase. The intensity of the Raman band around 280 cm^{-1} , which is one of the characteristic bands of the tetragonal phase, continuously decreased and approached zero between $X=90$ and 95 , which reflects the tetragonal-cubic phase boundary is located within this compositional range. The lattice distortion does not induce the cubic-tetragonal phase transition but an internal distortion in oxygen sublattice, oxygen displacement along the c_f axis from the ideal fluorite position, does.

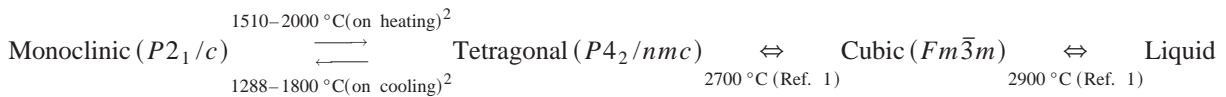
DOI: 10.1103/PhysRevB.64.134104

PACS number(s): 61.10.-i, 61.66.-f, 61.72.-y, 64.10.+h

I. INTRODUCTION

Hafnia-based (HfO_2) ceramics are some of the most interesting high-temperature materials in current technologies with many applications as well as zirconias (ZrO_2). Hafnia-based materials can be used in solid electrolytes for fuel cells, oxygen-gas sensors, refractories, coatings for oxidation resistance, control rods for a nuclear reactor, etc. Their physical and chemical properties relating to such uses strongly

depend on the crystal structures, especially phase transitions induced by internal distortions relating to oxygen displacement. Although hafnia-based ceramics have relatively simple crystal structures, their phase transitions and phase diagrams are not fully understood. The physical and chemical properties of HfO_2 are similar to those of ZrO_2 .¹⁻⁴ The structural phase transition of undoped HfO_2 also resembles that of undoped zirconia, although the transition point of HfO_2 is higher as shown by the following:



A temperature-composition phase diagram of the HfO_2 - CeO_2 system is shown in Fig. 1. This figure involves not only the stable phase boundaries (solid lines) but also metastable phase boundaries as T_0^{t-m} , $T_0^{t''-t'}$, and $T_0^{c-t''}$ shown by alternate long and short lines, where the gibbs energy of the tetragonal phase G_t equals that of the monoclinic phase G_m at a temperature T_0^{t-m} .⁷ t' and t'' forms are defined as compositionally homogeneous, metastable tetragonal phases that are formed diffusionlessly with a c_f/a_f ratio larger than unity and with an axial ratio of unity ($c_f/a_f=1$), respectively, where the suffix f denotes the pseudo-fluorite cell. Both tetragonal forms, t' and t'' , belong to space group $P4_2/nmc$ with oxygen displacements from an ideal fluorite position (Fig. 2, Table I).^{3,4} These forms are conveniently

distinguished from the stable t that formed diffusionally in the zirconia and hafnia solid solutions. The t'' form has been suggested in the diffusionless cubic-tetragonal ($c-t'$) phase change of the HfO_2 - $\text{RO}_{1.5}$ systems ($R=\text{Gd, Y, and Yb}$),^{3,4} as has been proposed in the ZrO_2 - CeO_2 (Refs. 15 and 16) and ZrO_2 - $\text{YO}_{1.5}$ (Refs. 17 and 18) systems. However, the precision of the axial ratio was not enough to support this suggestion because of the low resolution of the conventional x-ray experiment in previous works of hafnia solid solutions.^{3,5,6}

Since oxygen has a smaller x-ray scattering factor than hafnium, x-ray diffraction is not sensitive to the structural changes induced by oxygen displacements, although the difference between a_f and c_f lengths can easily be observed by this technique. In such a case, neutron diffraction and Raman

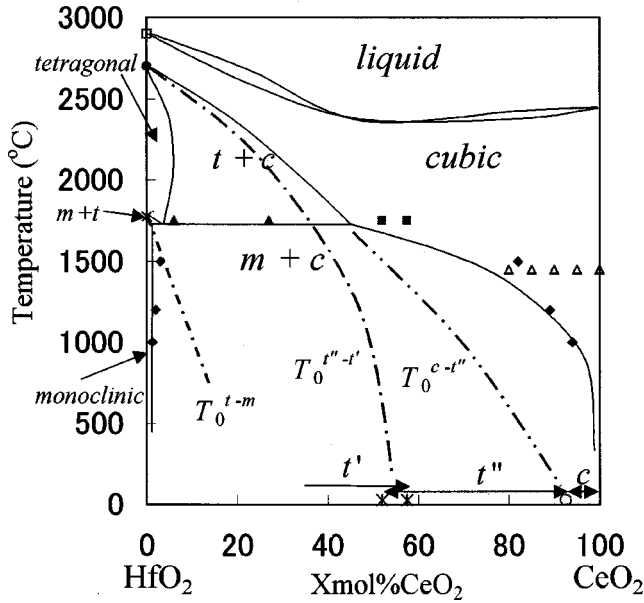


FIG. 1. Metastable-stable phase diagram in the $\text{HfO}_2\text{-CeO}_2$ system; solidus, \square (Ref. 1); monoclinic / (monoclinic+cubic) / cubic stable phase boundaries, \blacklozenge (Ref. 5); tetragonal/(tetragonal+cubic)/cubic stable phase boundaries, \blacktriangle (Ref. 6); cubic stable phase, \blacksquare (Ref. 6), \triangle (present work, see the section II A); T_0^{t-m} , \times (Ref. 2); T_0^{t-c} , \bullet (Ref. 1); $T_0^{t'-t''}$, $*$ (Ref. 6); $T_0^{c-t''}$, \circ (present work). Stable phase boundaries and metastable boundaries are shown by solid lines and alternate long and short lines, respectively. Metastable compositionally homogeneous phases obtained by rapid quenching are indicated at lower margin.

scattering can be powerful tools that are sensitive to oxygen atoms. However, HfO_2 systems are unfortunately not appropriate for a neutron study because they absorb neutrons very largely. On the other hand, Raman scattering is one of the most powerful tools for observing the cubic-tetragonal phase change induced by oxygen displacements in the $\text{HfO}_2\text{-CeO}_2$ system. Recently, by means of Raman spectroscopy, we have observed a phase transition between the cubic and tetragonal phases in centrosymmetric SrZrO_3 perovskite caused by cooperative oxygen-octahedron tilting (distortion).¹⁹ Both x-ray diffraction and Raman scattering techniques, which were successfully performed in this study, are crucial to understand this type of phase changes. Especially, the synchrotron high-resolution x-ray-diffraction technique was used to obtain more precise measurements of c_f/a_f in the $\text{HfO}_2\text{-CeO}_2$

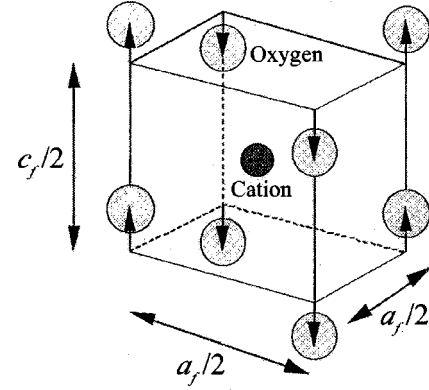


FIG. 2. Atomic configuration of the tetragonal phase with an axial ratio of c_f/a_f unity (t'' form). Oxygen atoms displace alternatively along the c_f axis (Arrows), but the lattice parameters a_f and c_f are equal. The symmetry of the cation sublattice is high but that of anion sublattice is low.

system in the present work. This study provides crucial information for understanding physical models concerning the role played by oxygen in the internal-distortion feature.

II. EXPERIMENTS AND DATA ANALYSIS

A. Sample preparation

It is important to use compositionally homogeneous samples for the study of the metastable phase change. The samples used for data collection were all prepared from commercially available $\text{HfOCl}_2 \cdot 8\text{H}_2\text{O}$ (containing 0.70-wt. % Zr; High-Purity Chemical Co. Ltd.) and $\text{Ce}(\text{NO}_3)_3 \cdot 6\text{H}_2\text{O}$ (Daiichi-Kigenso Chemical Co. Ltd.). The $\text{HfOCl}_2 \cdot 8\text{H}_2\text{O}$ and $\text{Ce}(\text{NO}_3)_3 \cdot 6\text{H}_2\text{O}$ powders were dissolved in approximately 1 N of HCl and 0.3 N of HNO_3 , respectively. A mixture of the HCl solution with Hf and the HNO_3 solution containing Ce was coprecipitated by being dropped in ammonia water. Coprecipitated hydroxide thus obtained was washed with diluted ammonia water and then dried at 100°C for 24 h. The powders were calcined at 1450°C for 5 h after being pressed into pellets. To maintain the homogeneity of the samples, they were then quenched by being dropped in water. The quenched products were crushed and ground again into powder. This quenched powder had a dark-gray color due to oxygen deficiency. To restore their oxygen content, defective $(\text{Hf, Ce})\text{O}_{2-\delta}$ was annealed in air at 600°C for 5 h. The powder then had a pale-yellow color due to oxygen stoichiometry.

TABLE I. Symmetries and Raman active modes of the polymorphs.

Form	Space group	Raman active mode	Oxygen displacement	Axial ratio c_f/a_f	Ref.
Monoclinic (m)	$P2_1/c$	$9A_g + 9B_g$	—	—	8–10
Tetragonal (t')	$P4_2/nmc$	$A_{1g} + 2B_{1g} + 3E_g$	Existing	>1	9–12
Tetragonal (t'' or c) ^a	$P4_2/nmc$	$A_{1g} + 2B_{1g} + 3E_g$	Existing	$=1$	9–12
Cubic (c)	$Fm\bar{3}m$	T_{2g}	Nonexisting	$=1$	8, 9, 13

^aIn x-ray-diffraction study (Ref. 14) both t'' and c forms were tentatively called as c form, because x-ray-diffraction cannot distinguish them from each other. Raman scattering enables us to distinguish between them.

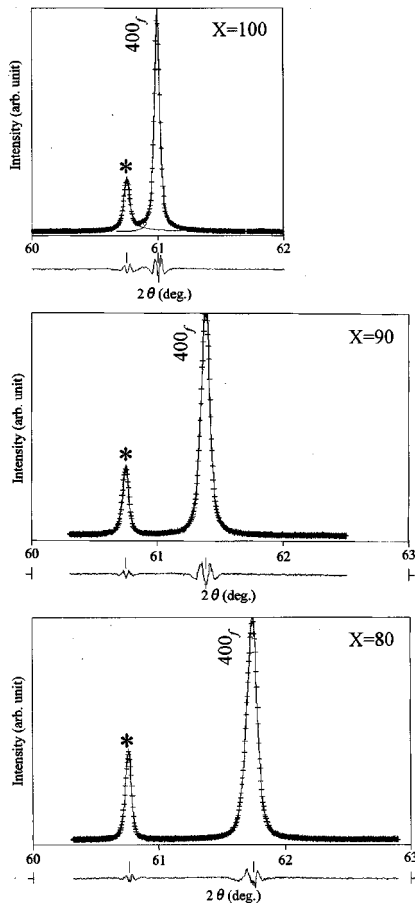


FIG. 3. Observed (+) and calculated (solid line) powder-diffraction profiles for 400_f reflection peaks of HfO_2 - X -mol %- CeO_2 and 400 reflection peaks of NBS Si(*).

B. Synchrotron x-ray powder diffraction

The samples used for x-ray diffraction measurements were well mixed with a NIST Si powder ($a = 5.430940 \text{ \AA}$ at 298.1 K) for angular calibration. To obtain x-ray-diffraction patterns with high resolutions and accurate numerical statistics, the synchrotron x-ray powder diffraction experiments were carried out by using the triple-axis/four-circle diffractometer²⁰ at the beamline BL-3A of the Photon Factory, KEK.²¹ A revolving sample stage was used to avoid the

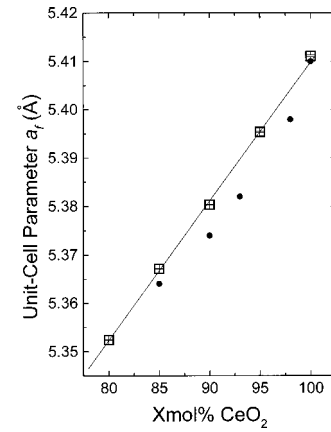


FIG. 4. Variation of the unit-cell parameter a_f with CeO_2 content X . \square , present work; \bullet , Spiridonov, Chyong, and Komissarova (Ref. 5).

effect of preferred-orientation of the crystal. The wavelength of incident x-ray monochromatized by an Si monochromator was $1.37879(4) \text{ \AA}$, which was determined by measuring the 16 reflection profiles of a NIST CeO_2 powder ($a = 5.41129 \text{ \AA}$ at 298.15 K). All measurements were performed at 293.65 K. The values of the lattice parameters of NIST Si and CeO_2 calculated at 293.65 K by considering their thermal expansion^{22,23} were used. The scanning conditions under which the splitting between 004_f and 400_f reflection peaks was investigated were $60^\circ \leq 2\theta \leq 63^\circ$, $\Delta 2\theta = 0.005^\circ$, and the measuring period was 8 s, where hkl_f was indexed on the basis of a pseudofluorite cell. The diffraction profiles for the 004_f and 400_f reflections were analyzed by assuming the Pearson-VII-type function.²⁴

C. Raman scattering

The existing phases of specimens were also investigated by Raman scattering, which is sensitive to oxygen displacements due to the large polarizability of oxygen.²⁵ Raman spectra were obtained using a Raman system (Atago-Jobin Yvon T64000, Japan-France) with a triple spectrometer and a charge-coupled device detector.²⁵ The Raman spectra were measured by using an Ar-ion laser source of 488.0 nm to avoid any luminescence from the specimens.^{4,15,18} Pattern

TABLE II. Crystal data, unit-cell parameters, and Raman peak intensities of HfO_2 - X -mol %- CeO_2 samples.

X	80	85	90	95	100
Space group	$P4_2/nmc$	$P4_2/nmc$	$P4_2/nmc$	$Fm\bar{3}m$	$Fm\bar{3}m$
Form	t''	t''	t''	c	c
$a_f = c_f$ (\AA) ^a	5.3524(1)	5.3671(1)	5.3803(1)	5.3954(1)	5.4111(2)
b	5.352(4)	5.367(4)	5.380(3)	5.395(3)	5.411(2)
c_f/a_f ^a	1.00000 ± 0.00003	1.00000 ± 0.00003	1.00000 ± 0.00004	1.00000 ± 0.00004	1.00000 ± 0.00004
b	1.000 ± 0.001	1.000 ± 0.002	1.000 ± 0.001	1.0000 ± 0.0008	1.0000 ± 0.0007
I_3/I_4 ^c	0.0193(4)	0.0088(3)	0.0018(2)	0	0

^aObtained by using the estimated standard deviation of peak position.

^bEstimated from the full width at half maximum of the 400_f reflection peak.

^c I_i denotes the i th Raman peak integrated intensity.

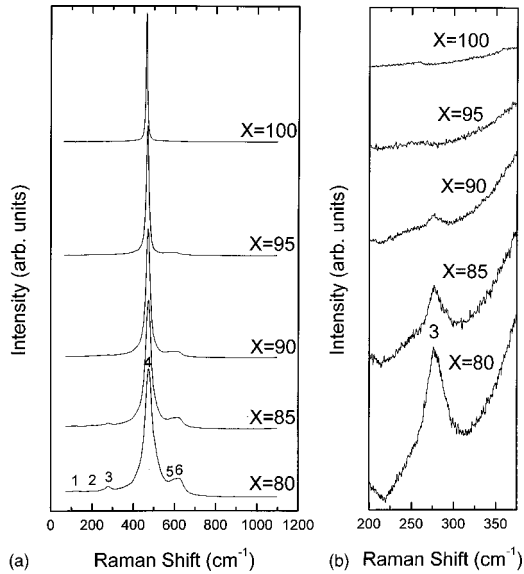


FIG. 5. (a) Raman spectra of HfO_2 - X -mol %- CeO_2 specimens, where the Raman shift was calibrated by using the position of an Hg line. (b) The third Raman band around 280 cm^{-1} , which is one of the characteristic bands of the tetragonal phase.

decomposition of the Raman spectra was performed by using the commercial profile-fitting program “GRAMS” and assuming Lorentz functions.

III. RESULTS AND DISCUSSION

Existing phases in HfO_2 - X -mol %- CeO_2 specimens were investigated by high-resolution x-ray diffraction and Raman scattering. The synchrotron x-ray-diffraction data of HfO_2 - X -mol %- CeO_2 samples ($X=80, 85, 90, 95,$ and 100) show that the 400_f reflection peaks have neither split into 004_f and 400_f peaks nor developed shoulders which might appear when some lack of homogeneity (Fig. 3). With an increase in CeO_2 content X , the unit-cell parameter a_f increased linearly, suggesting compositional homogeneity according to Vegard’s law (Fig. 4). The c_f/a_f values for all samples were estimated to be unity. The precision of the c_f/a_f ratio for all samples was estimated to be less than ± 0.00004 from the estimated standard deviation of the peak position and to be less than ± 0.002 from the full width at half maximum of the 400_f reflection peak (Table II). On the other hand, the Raman spectra of samples of $X=80, 85,$ and 90 revealed the tetragonal phase. According to the symmetry analysis, the cubic and tetragonal phases have one and six Raman-active modes, respectively (Table I). In particular, the first three bands in Fig. 5(a) cannot be explained by the cubic phase. The third Raman band around 280 cm^{-1} , which is one of the characteristic bands of the tetragonal phase,^{4,15,18} appeared clearly in samples of $X=80, 85,$ and 90 [Fig. 5(b)]. Peaks 5 and 6 will be induced by a defect structure occurring by the substitution of Hf cation for Ce.¹⁵ The fourth peak did not change greatly with X . Because the Raman peak area ratio I_3/I_4 has been reported to be proportional to oxygen displacements revealed by neutron diffraction,^{15,16} the Raman peak area ratio I_3/I_4 plotted in Fig. 6 can be used to

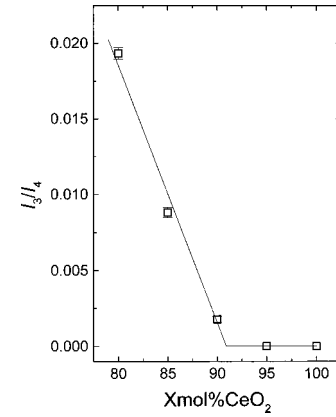


FIG. 6. Variation of integrated intensity ratio I_3/I_4 of Raman bands with CeO_2 content.

clearly show the tetragonal-cubic phase boundary. The integral intensity ratio I_3/I_4 continuously decreased with X and became mostly 0 between $X=90$ and 95 , where the tetragonal-cubic phase boundary was located. X-ray powder diffraction indicated that the axial ratio c_f/a_f equaled unity in HfO_2 - X -mol %- CeO_2 samples ($X=80, 85, 90, 95,$ and 100). These results strongly suggest the existence of the tetragonal form (t'' form) with an axial ratio c_f/a_f of unity but having oxygen displacements along the c_f axis as the intermediate form between cubic (c) and tetragonal (t') phases, which is observed in HfO_2 - X -mol %- CeO_2 samples ($X=80, 85,$ and 90) (Table II). The cubic-to-tetragonal phase transition is not induced by the lattice distortion, elongation of c_f axis and/or shrinkage of the a_f axis, but by the internal distortion, displacement of oxygen ions along the c_f axis from the ideal fluorite site ($8c$ site in $Fm\bar{3}m$).

The t'' and t' forms belong to the same space group ($P4_2/nmc$). However, the t'' form should be distinguished from the t' form because a thermal barrier exists between these form as follows. The t'' - t' change was studied by x-ray diffraction and the coexistence of t'' and t' forms was observed in the HfO_2 - CeO_2 system (symbol* in Fig. 1).⁶ It was also found that a hysteresis exists between t'' and t' forms.¹⁴ (In the x-ray diffraction study in Ref. 14, both t'' and c forms were tentatively called as c form, because only the x-ray diffraction studies could not distinguish them from each other. Raman scattering, on the other hand, enables us to distinguish them.) Thus, a thermally activated process is necessary for the t'' - t' change to occur due to a lattice strain, which increases the axial ratio c_f/a_f against the t'' matrix. These results indicate that t'' - t' change is first order. In contrast to this change, the intensity I_3/I_4 of Raman spectra continuously decreased and approached zero as X increased (Fig. 6), which can be interpreted as the t'' -form structure continuously approaching that of the cubic phase. No hysteresis was reported for the t'' and cubic phase transition.¹⁵ Since the internal distortion, the displacement of oxygen ions from the ideal fluorite site, does not induce strains, no activated process may be necessary for the c - t'' phase transition. These observations suggest that the c - t'' phase transition is first order near second one. The c - t' phase transition can also be interpreted as the sublattices of anion and cation.

Some materials belonging to the fluorite family with the general formula AB_2 have different phase-transition temperatures between the sublattices of anion and cation. For example, those of $(\text{Ba}, \text{Sr}, \text{Ca})\text{F}_2$,²⁶ PbF_2 ,²⁷ and $\text{Zr}(\text{Ca}, \text{Y})\text{O}_{2-x}$ ²⁸ have been reported. Thus, we strongly believe, it is not unusual that a phase comprising both high-symmetric cation sublattice and low-symmetric anion sublattice (t'' form) exists.

IV. CONCLUDING REMARKS

In the present study we confirmed the existence of the tetragonal form (t'' form) with an axial ratio c_f/a_f of unity in HfO_2 - X -mol % - CeO_2 samples ($X=80, 85,$ and 90) by means of high-resolution synchrotron x-ray diffraction and Raman scattering, although generally the a_f axis should not be equal to the c_f axis in a tetragonal system. The c_f/a_f ratio

for these samples was estimated to be 1 ± 0.00004 from the estimated standard deviation of the peak position and to be 1 ± 0.002 from the full width at half maximum of the 400_f reflection peak. We must now recognize the existence of oxygen displacement and consider the very weak Raman band of the tetragonal structure to determine its symmetry. The internal distortion, the oxygen displacement along the c_f axis from the ideal fluorite position, induces the symmetrical change from cubic to tetragonal, but it does not induce lattice distortion. The above-mentioned concept would help to explain the structure-property correlation in such materials.

ACKNOWLEDGMENTS

The authors thank Dr. O. Yokota, Mr. S. Koura, and Mr. T. Kato for their help with experiments at the Photon Factory.

*Present address: Department of Advanced Materials Science and Engineering, Faculty of Engineering, Yamaguchi University, 2-16-1, Tokiwadai, Ube-shi, Yamaguchi 755-8611, Japan.

†Present address: Department of Materials Science and Engineering, Interdisciplinary Graduate School of Science and Engineering, Tokyo Institute of Technology, Nagatsuta 4259, Midori-ku, Yokohama 226-8502, Japan.

‡Author to whom correspondence should be addressed: Materials and Structures Laboratory, Tokyo Institute of Technology, Nagatsuta 4259, Midori-ku, Yokohama 226-8503, Japan. FAX: +81-45-924-5358. Email address: yoshimu1@rlem.titech.ac.jp

¹C. T. Lynch, in *High Temperature Oxides* edited by A. M. Alper (Academic, New York, 1970), Vol. 5, Part II, pp. 193–216.

²D. R. Wilder, J. D. Buckley, D. W. Stacy, and J. K. Johnstone, *Colloq. Int. C. N. R. S.* **205**, 335 (1971).

³M. Yashima, T. Hirose, M. Kakihana, Y. Suzuki, and M. Yoshimura, *J. Ceram. Soc. Jpn.* **103**, 622 (1995).

⁴M. Yashima, H. Takahashi, K. Ohtake, T. Hirose, M. Kakihana, H. Arashi, Y. Ikuma, Y. Suzuki, and M. Yoshimura, *J. Phys. Chem. Solids* **57**, 289 (1996).

⁵F. M. Spiridonov, L. K. Chyong, and L. N. Komissarova, *Russ. J. Inorg. Chem. (transl. of Zh. Neorg. Kh.)* **22**, 327 (1977).

⁶A. M. Gavrish, E. I. Zoz, N. V. Gul'ko, and A. E. Solov'eva, *Inorg. Mater. (transl. of Neorg. Mater.)* **11**, 574 (1975).

⁷M. Yashima, M. Kakihana, and M. Yoshimura, *Solid State Ionics* **86–88**, 1131 (1996).

⁸W. B. White, *Mater. Res. Bull.* **2**, 381 (1967).

⁹V. G. Keramidias and W. B. White, *J. Am. Ceram. Soc.* **57**, 22 (1974).

¹⁰D. Michel, M. Perez Y Jorba, and R. Collongues, *J. Raman Spectrosc.* **5**, 163 (1976).

¹¹D. P. C. Thackeray, *Spectrochim. Acta, Part A* **30**, 549 (1974).

¹²M. Ishigame and T. Sakurai, *J. Am. Ceram. Soc.* **60**, 367 (1977).

¹³P. G. Marlow, J. P. Russell, and J. R. Hardy, *Philos. Mag.* **14**, 409 (1966).

¹⁴M. Yashima, K. Morimoto, N. Ishizawa, and M. Yoshimura, *J. Am. Ceram. Soc.* **76**, 2865 (1993).

¹⁵M. Yashima, H. Arashi, M. Kakihana, and M. Yoshimura, *J. Am. Ceram. Soc.* **77**, 1067 (1994).

¹⁶M. Yashima, S. Sasaki, Y. Yamaguchi, M. Kakihana, M. Yoshimura, and T. Mori, *Appl. Phys. Lett.* **72**, 182 (1998).

¹⁷M. Yashima, S. Sasaki, M. Kakihana, Y. Yamaguchi, H. Arashi, and M. Yoshimura, *Acta Crystallogr., Sect. B: Struct. Sci.* **50**, 663 (1994).

¹⁸M. Yashima, K. Ohtake, M. Kakihana, H. Arashi, and M. Yoshimura, *J. Phys. Chem. Solids* **57**, 17 (1996).

¹⁹H. Fujimori, M. Yashima, M. Kakihana, and M. Yoshimura, *Phys. Rev. B* **61**, 3971 (2000).

²⁰K. Kawasaki, Y. Takagi, K. Nose, H. Morikawa, S. Yamazaki, T. Kikuchi, and S. Sasaki, *Rev. Sci. Instrum.* **63**, 1023 (1992).

²¹S. Sasaki, T. Mori, A. Mikuni, H. Iwasaki, K. Kawasaki, Y. Takagi, and K. Nose, *Rev. Sci. Instrum.* **63**, 1047 (1992).

²²Y. S. Touloukian, R. K. Kirby, R. E. Taylor, and T. Y. R. Lee, in *Thermophysical Properties of Matter, Thermal Expansion Non-metallic Solids*, Vol. 13 (IFI/Plenum, New York, 1977), p. 154.

²³B. T. Kilbourn, in *Cerium: A Guide to Its Role in Chemical Technology* (Molycorp, White Plains, NY, 1992), p. 12.

²⁴H. Toraya, *J. Appl. Crystallogr.* **19**, 440 (1986).

²⁵M. Kakihana, M. Yashima, M. Yoshimura, L. Borjesson, and M. Kall, *Trends in Applied Spectroscopy* (Council of Scientific Research Integration, Trivandrum, India, 1993), Vol. 1, pp. 261–311.

²⁶M. W. Thomas, *Chem. Phys. Lett.* **40**, 111 (1976).

²⁷S. Palchoudhuri and G. K. Bichile, *Solid State Commun.* **67**, 553 (1988).

²⁸J. Faber, Jr., M. H. Mueller, and B. R. Cooper, *Phys. Rev. B* **17**, 4884 (1978).